Biologically inspired LED lens from cuticular nanostructures of firefly lantern

Jae-Jun Kim[a], Youngseop Lee[a], Ha Gon Kim[b], Ki-Ju Choi[c], Hee-Seok Kweon[c], Seongchong Park[d], and Ki-Hun Jeong[a,1]

[a]Department of Bio and Brain Engineering and KAIST Institute for Optical Science and Technology, Korea Advanced Institute of Science and Technology, Yuseong-gu, Daejeon 305-701, Republic of Korea; [b]Firefly Institute, Culture and Tourism Division, Muju-eup, Muju-gun, Jellobuk-do 568-701, Republic of Korea; [c]Division of Electron Microscopic Research, Korea Basic Science Institute, Yuseong-gu, Daejeon 305-806, Republic of Korea; and [d]Division of Physical Metrology, Korea Research Institute of Standards and Science, Yuseong-gu, Daejeon 305-340, Republic of Korea

Cuticular nanostructures found in insects effectively manage light for light polarization, structural color, or optical index matching within an ultrathin natural scale. These nanostructures are mainly dedicated to manage incoming light and recently inspired many imaging and display applications. A bioluminescent organ, such as a firefly lantern, helps to out-couple light from the body in a highly efficient fashion for delivering strong optical signals in sexual communication. However, the cuticular nanostructures, except the light-producing reactions, have not been well investigated for physical principles and engineering biomimetics. Here we report a unique observation of high-transmission nanostructures on a firefly lantern and its biological inspiration for highly efficient LED illumination. Both numerical and experimental results clearly reveal high transmission through the nanostructures inspired from the lantern cuticle. The nanostructures on an LED lens surface were fabricated by using a large-area nanotemplating and reconfigurable nanomolding with heat-induced shear thinning. The biologically inspired LED lens, distinct from a smooth surface lens, substantially increases light transmission over visible ranges, comparable to conventional antireflection coating. This biological inspiration can offer new opportunities for increasing the light extraction efficiency of high-power LED packages.

firefly light organ | antireflective structures | nanostructures on lens | light-emitting diode

Cuticular nanostructures of insects provide many intriguing photonic functions in polarization (1–3), structural color (4–8), and antireflection (9–16). Elytron of beetles selectively reflects left circularly polarized light. The polarized light is caused by chiral and periodic structures with helicoidal orientation. Wing scales of butterflies reflect the iridescent structural color. The structural color varies with diverse spectral properties depending on the angle of incidence because of the optical interference with multilayer reflector. Antireflective structures found on the corneas of moth eyes can provide high photon collection to facilitate nocturnal bustle (9, 10). The nanostructures can reduce light reflection by matching optical impedance with subwavelength nanostructures. Not only on insects' eyes, antireflective structures with high transmission are also found on insects' wings for camouflaging of diurnal activity (15, 16). The photonic functions reported in previous works are mainly dedicated to managing incoming light.

Recently, these cuticular nanostructures have been used as inspiration for many imaging and display applications. The polarization structures have been mimicked with deposition of birefringent and chiral materials (2). The structural color structures have also been mimicked with 3D photonic crystals by using nanocasting lithography (5), focused ion-beam chemical vapor deposition (6), conformal-evaporated film-by-rotation techniques (7), and soaking methods (8). In addition, the antireflective structures have been mimicked with nanonipple arrays by using interference lithography (11), e-beam lithography (12), self-masked dry etching (13), nanoimprint (14–16), and bio-templates (15, 16). However, most previous works were restricted to planar

emulation with low yield and limited to managing incoming light from the outside through the nanostructures for diverse imaging and display applications.

Nature also implements such similar structures for out-coupling bioluminescent light from the body. In particular, a firefly lantern is a distinctive organ for delivering optical signals in sexual communication. When fireflies communicate with each other for mating, males emit courtship signals to females, which selectively reply with their own response flash. Highly efficient emission of bioluminescent light is the first-order basic requirement for successful communication for sexual selection. A firefly light organ (also called a "lantern"), found in either the fifth abdominal segments in females or the fifth and sixth in males, has different photonic layers with subsequent arrangement. The lantern organ encloses around the abdomen and consists of a cuticle, a photogenic layer, and a dorsal layer within around 100 μm in thickness (17, 18). The unique anatomical features are apparently associated with highly efficient illumination of bioluminescent light. For example, the photogenic layer plays an important role for light producing reaction with high quantum yield of ~41% (19). However, the photonic functions of dorsal or cuticle layers were not well concluded and little effort on engineering biomimetics for illumination has been made yet.

This work reports an engineering inspiration of the cuticular nanostructures found in a firefly lantern. The light organs exist on the abdominal segments of a firefly (*Luciola lateralis* Motschulsky) in males, as shown in Fig. 1*B*. Unlike the normal (N), the lantern (L) cuticle has longitudinal nanostructures with a highly ordered arrangement along the sagittal plane of a firefly body (Fig. 1 *C–E*). The physical dimensions were statistically extracted from the SEM images. The period, height, and width roughly range near 250 nm, 110 nm, and 150 nm, respectively. For further investigation, the bioluminescent spectra were measured with a microscopic spectrometer and the result shows a center wavelength of 563 nm in males (68 nm in bandwidth). The transmittance of bioluminescent light ($\lambda = 560$ nm) through the lantern cuticle was calculated by using a finite difference time domain (FDTD) method (Fig. 1*F*). The refractive index of chitin as cuticle medium (reported value: 1.56) (20) was chosen for this FDTD calculation. The maximum transmission are clearly shown at 250 nm in period, 150 nm in width, and 110 nm in height, very similar to what is observed in nature. The nanostructured surface serves as a single layer with the calculated effective refractive index of roughly 1.24 (21), the thickness of which matches well
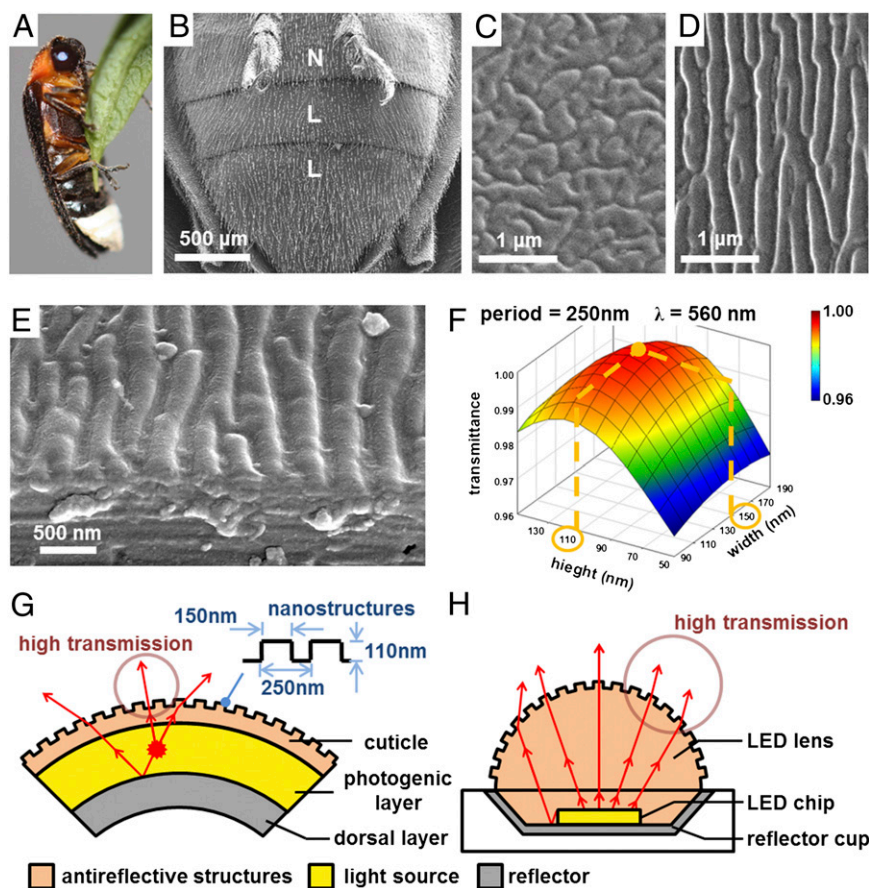
Fig. 1. Engineering inspiration from highly ordered cuticular nanostructures of a firefly light organ. (*A*) The optical image of a firefly (*L. lateralis* Motschulsky) in male. The SEM images of (*B*) abdominal segments of a firefly in male including normal (N) and lantern (L) cuticles, (*C*) amorphous nanostructures on the normal cuticle, (*D*) highly ordered nanostructures on the lantern cuticle and (*E*) a transverse cross-section of the light organ. (*F*) Transmission of bioluminescent light (λ = 560 nm) through nanostructured surfaces on the lantern cuticle calculated by the FDTD method. The results show the maximum value at 250 nm in period, 150 nm in width, and 110 nm in height, very similar to natural one. This result clearly explains that the highly ordered cuticular nanostructures surrounding the ventral photogenic layer contribute to high extraction of bioluminescent light outside the lantern cuticle. Anatomical comparisons between (*G*) a firefly lantern and (*H*) a high-power LED package. Inspired from a firefly lantern comprising a dorsal layer, a photogenic layer, and a cuticle, a high-power LED package has a similar configuration of a reflector cup, an LED chip, and a lens with nanostructures. Like the cuticular nanostructures of a firefly lantern, the nanostructures on LED lens surfaces can serve as highly efficient extraction of the LED light for a high-power LED package.

with a quarter wavelength over the square root of refractive index in cuticular medium (i.e., the antireflection condition). This result indicates that the highly ordered cuticular nanostructures surrounding the ventral photogenic layer play an important role for reducing the index mismatch between air and the cuticle surface for high light extraction of bioluminescent light. For an anatomical perspective, a firefly lantern consists of a dorsal layer, a photogenic layer, and a cuticle (Fig. 1*G*). The photogenic layer emits bioluminescent light in all directions. The light passes through the cuticle either directly or after reflecting off the dorsal layer, which is located under the photogenic layer and also known as a dielectric mirror (17, 18, 22). The natural design can inspire the configuration of high-power LED packages. High-power LED packages also have a similar configuration of a reflector cup, an LED chip, and a lens (Fig. 1*H*). The LED chip emits light with Lambertian distribution. Some light directly passes through the lens; other light is reflected from the reflector cup and finally extracted through the lens. Like the cuticle nanostructures of a firefly lantern, the nanostructures on the LED lens surfaces can help to efficiently extract the LED light by reducing the optical impedance between air and lens material. Note that the bio-inspired nanostructures were selected as honeycomb-packed nanopillars to minimize birefringence because of

uniaxial anisotropy in an effective refractive index, unlike a natural one with a longitudinal shape.

Results and Discussion

The cuticular nanostructures of a firefly lantern were mimicked by implementing the nanostructures on a curved lens surface. The nanofabrication was done by colloidal lithography, reactive ion etching (RIE), and reconfigurable nanomolding with heat-induced shear thinning (Fig. 2*A*). A UV curable optical resin (refractive index = 1.56) very similar to the refractive index of chitin was used as lens material. First, a large area nanotemplate with nanopillars (4 cm²) was fabricated by colloidal lithography and RIE (Fig. 2*A*, step I). In colloidal lithography, polystyrene nanospheres were spin-coated with a honeycomb-packed mono-layer on a thermally oxidized silicon substrate. The period between nanopillars was determined by the diameter of nanospheres. The width and height were controlled by isotropically etching the nanospheres with oxygen plasma and then by anisotropically etching silicon dioxide with the nanosphere mask. Polystyrene nanospheres on the nanotemplate were removed with oxygen plasma and piranha cleaning. Antistiction film was deposited on the nanopillars by using fluorocarbon-based plasma. A 100-μm thick polydimethylsiloxane (PDMS) was spin-coated on the nanotemplate. The thin PDMS was thermally cured at 150 °C for
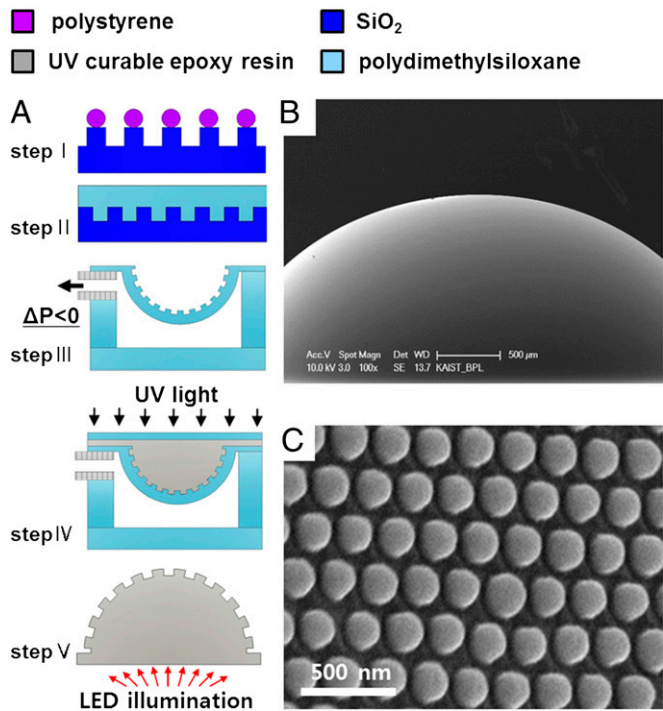
Fig. 2. The nanofabrication procedures and the SEM images of a biologically inspired LED lens. (*A*) A large area nanotemplate by colloidal lithography and reactive ion etching (step I). Thin PDMS replication of nanostructures by heat induced shear thinning (at 150 °C) (step II). The LED lens template by deforming the thin PDMS membrane under a negative pressure drop (step III). A UV-curable optical resin recast the curved PDMS membrane with nanostructured surface (step IV). The LED lens was released from the thin PDMS membrane (step V). (*B*) A biologically inspired LED lens (lens diameter 4.4 mm). (*C*) Highly ordered nanostructures arrays are spherically arranged on a polymer dome lens surface.

30 min on a hot plate (Fig. 2*A*, step II) to reduce the viscosity of the PDMS prepolymer. Note that this heat-induced shear thinning effectively improves the PDMS replication fidelity of such highly dense nanostructures (i.e., height = 80∼140 nm, width = 150 nm, period = 250 nm) (Figs. S1 and S2). This PDMS replica is counterbalanced with negative tone (i.e., from nanopillars to nanoholes) to avoid easy collapse of PDMS nanostructures because of the relatively low elastic modulus of PDMS (23). The thin PDMS membrane with nanohole arrays was permanently bonded with a thick PDMS slab by oxygen plasma treatment and then released from the nanotemplate. The lens template was prepared by deforming the thin PDMS membrane under a negative pressure drop (Fig. 2*A*, step III). A UV-curable optical resin recast the curved PDMS membrane with nanostructures under UV exposure (Fig. 2*A*, step IV). Finally, the polymer LED lens with nanostructured surface was released from the thin PDMS membrane (Fig. 2*A*, step V). Fig. 2*B* shows a SEM image of the polymer lens with a nanostructured surface (4.4 mm in lens diameter). Highly ordered nanostructure arrays (250 nm in period, 150 nm in width, and 120 nm in height) are spherically arranged on a hemispherical polymer lens surface (Fig. 2*C*).

Light transmission through a polymer LED lens with nanostructured surface was experimentally characterized. The atomic force microscope (AFM) images show the nanostructures with four different heights at constant period and width (height = 80, 100, 120, 140 nm at period = 250 nm and width = 150 nm) on a UV-curable optical resin (Fig. 3*A*). The results demonstrate the nanostructures on the lens surface were faithfully transferred from the nanotemplates with four different heights during two-

step replications (i.e., silicon dioxide to PDMS and PDMS to UV curable resin). The optical images exhibit light reflection from the five different LED lens surfaces under a constant illumination angle from a white-light fluorescent lamp (Fig. 3*B*). The
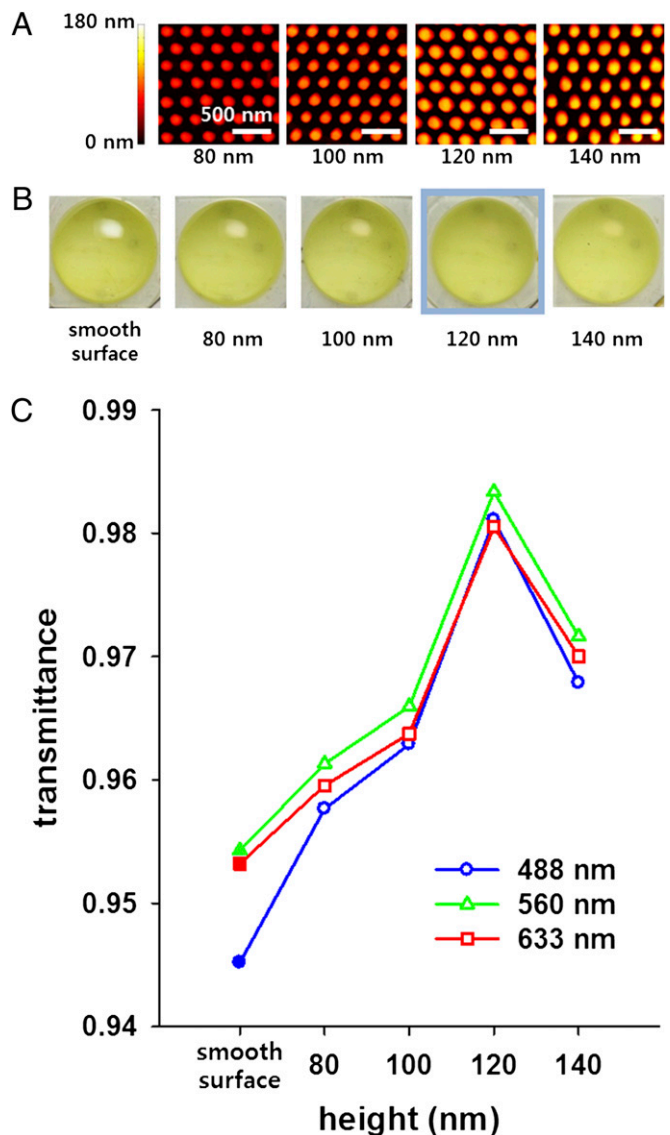

Fig. 3. Light transmission through the LED lenses with nanostructures of different heights. (*A*) AFM images of the nanostructures with four different heights at constant period and width (height = 80, 100, 120, 140 nm at period = 250 nm and width = 150 nm) on a UV-curable optical resin. The nanostructures on lens surface were faithfully transferred from the nanotemplates with four different heights during two steps replications (i.e., silicon dioxide to PDMS and PDMS to UV curable resin). (*B*) Light reflection from the five different LED lens surfaces. The optical images were captured at a constant illumination angle from a white-light fluorescent lamp. The minimum reflection is clearly shown from the LED lens with height at 120 nm. The nanostructures on lens surface obviously serve as antireflective structures. (*C*) Light transmission through the nanostructured LED lenses with different pattern heights and a smooth surface LED lens. The measured results show the nanostructured lenses have higher transmittance than a smooth surface lens over a full range of visible wavelengths. The transmittance is maximized at 120 nm in height. In particular, the maximum spectral transmittance is shown at 560 nm, corresponding to the center wavelength of a bioluminescent light from a firefly. Both the calculated and measured results clearly reveal the highly ordered nanostructures on a firefly light organ substantially contribute to high transmission.

minimum reflection is clearly shown from the LED lens with a height at 120 nm (i.e., biologically inspired LED lens). The nanostructures on the lens surface obviously serve as antireflective structures. Light transmission through the LED lenses was measured with an integrating sphere with an LED light source and a fiber-coupled spectrometer (Spectral Products SM640). All of the lenses were measured with a single LED chip to avoid the measurement errors caused by the flux variation between different LED chips. The LED lenses with a nanostructured surface clearly show high transmission over a full range of visible wavelengths, compared with that of a smooth surface lens (Fig. 3C). The calculated and measured results show that the maximum transmittance is shown at ~120 nm in height. In particular, the maximum spectral transmittance is 0.983 at 560 nm in wavelength, which corresponds to the center wavelength of bioluminescent light from a firefly. In addition, the nanostructured surface shows even lower light reflection at the optical resin-air interface than that of conventional single-layer adhesive resin coating of magnesium fluoride (24). Considering that Fresnel reflection of the smooth surface is ~0.048 at normal incidence, this improvement is apparently significant in transmission. This improvement is visibly observed in the reflection from the lens surface (Movie S1). The results clearly reveal the highly ordered nanostructures on a firefly light organ substantially contribute to high transmission.

Light transmission through the biologically inspired LED lens (i.e., lens with nanostructures of 120 nm in height) is very sensitive to both the lens curvature and the LED emitting angle. In this experiment, the biologically inspired LED lens was prepared with four different lens curvatures. The lens transmission significantly depends on the degree of normal incidence (DNI); that is, the ratio of a near normal incidence angle to lens surface over the total emitting angle of an LED light source. The near normal incidence angle was defined by less than 3° for convenience. The side views of lenses show that DNI increases with the radius of lens curvature (ROC). For example, the lens surface of 4.5 mm in ROC becomes the same near normal incidence angle with the illumination LED angle (i.e., DNI = 1.0). The lens transmission for four different DNIs was also measured by using an integrating sphere coupled with a single LED chip of a constant LED emitting angle of ± 30°. The measured results show the lens transmittances for both smooth surface and biologically inspired LED lenses increase as DNI approaches 1. For an LED lens of 4.5 mm in ROC, the lens surface has near normal incidence for all rays from an LED light source (i.e., DNI = 1.0). The lens transmittance increases by 3% on average in a visible range (480 nm ~640 nm), which is comparable to the value on a planar surface (Fig. S3). These results clearly support that the biologically inspired LED lens has the maximum transmission when all rays from an LED light source are normally incident to the lens surface.

In summary, this work reports a unique observation of highly ordered cuticular nanostructures founded in a firefly lantern and a biologically inspired lens for highly efficient LED illumination. Both the calculated and measured results unveil that highly ordered nanostructures on the lantern cuticle substantially contribute to increase light transmission as a low index effective medium. The biologically inspired LED lens features the nanostructures on a curved lens surface. This lens demonstrates the maximum transmittance of 98.3% at 560 nm and also 3% over visible ranges higher than that of a smooth surface lens, also comparable to that of a conventional adhesive resin coating of magnesium fluoride. This biological inspiration can offer new opportunities for single-step and low-cost molded lenses with high transmission in high-power LED applications, such as liquid crystal display backlight units, mobile camera phone flashes, automotive, domestic, and medical lighting.

Materials and Methods

Firefly Sample Treatment and SEM Measurement. Adult fireflies of *L. lateralis* Motschulsky were obtained from the Muju Firefly Institute in Korea. The firefly samples were treated under sonication to remove contaminant and infiltrated with 2.3 M sucrose overnight. To obtain the cross-section of the firefly lantern, one of the samples was mounted on cryo-holder and quick-frozen (−196 °C). The holder was mounted on ultramicrotome (UC7; Leica). The sample was trimmed at −80 °C and sectioned at −120 °C. This sectioning step was not performed in observing the surface of cuticular nanostructures. The sample was washed in distilled water to remove sucrose and then dehydrated through ethanol solutions of 50%, 70%, 90%, and 95% (vol/vol) twice for 10 min each and 100% three times for 10 min. Subsequently, the sample was treated with hexamethyldisilazane (HMDS; EMS) and air-dried overnight. The sample was then attached to an aluminum SEM stub by using carbon tape. Thin platinum was coated on the sample surface using sputter (208HR; Cressington). A high-resolution field-emission scanning electron microscope (FE-SEM FEI) was used for analyzing the nanostructures of a firefly lantern.

Colloidal Lithography and Reactive Ion Etching. The nanotemplates were prepared by colloidal lithography and RIE. First, a 1-μm thick SiO_2 film was thermally grown on a 4-in Si (100) wafers. These wafers were cut into square pieces (3 × 3 cm²). These substrates were cleaned by immersion in piranha solution (10:1 H_2SO_4/H_2O_2) and rinsed repeatedly with deionized water. The substrates were dried in a stream of nitrogen and retreated with oxygen plasma (IHP-1000; APP). A 10% (wt) aqueous suspension of polystyrene nanospheres with 260 nm in diameter was purchased (Thermo Scientific). A colloidal monolayer of the nanospheres was prepared by spin-coating a 7.5% (wt) polystyrene colloidal solution at 500 rpm for 5 s and 3,000 rpm for 30 s onto the plasma-treated substrates. Although the size of the polystyrene nanosphere is 260 nm, the period of polystyrene nanospheres is
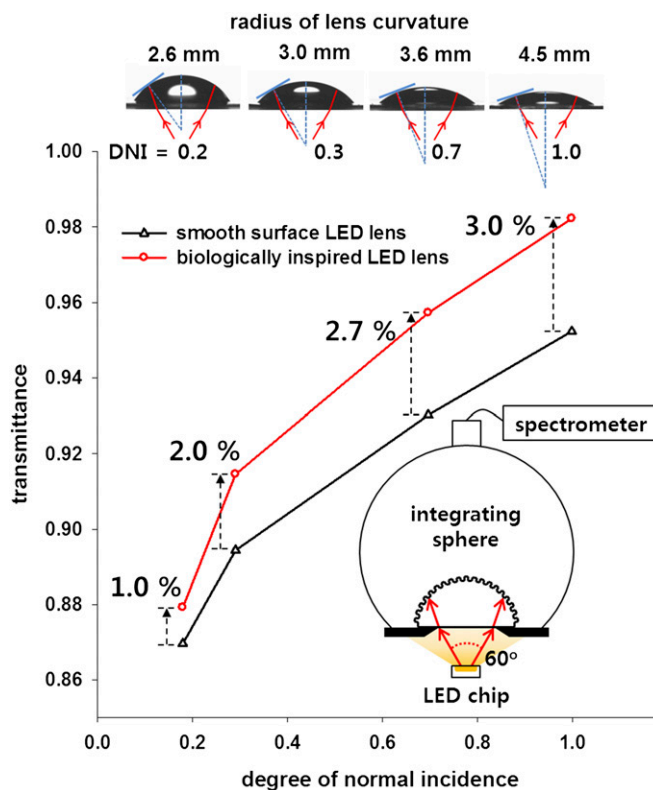
Fig. 4. Light transmission through the biologically inspired LED lens depending on lens curvatures under a constant LED emitting angle of ± 30°. DNI, the ratio of a near normal incidence angle to lens surface over total emitting angle of an LED light source, increases with the ROC. The biologically inspired LED lens shows the maximum transmission at DNI = 1.0; that is, the lens surface has near normal incidence for all rays from an LED light source (also corresponds to the LED lens of 4.5 mm in ROC).

about 250 nm because of close packing. The diameter of polystyrene nanospheres was controlled by a RIE equipment (Systa) with 50 standard cubic centimeters per minute (sccm) of oxygen and 150 sccm of argon at a pressure of 270 mTorr and radio frequency power of 150 W for 24 s. Nanostructures of the nanotemplate were anisotropically defined by dry-etching with 15 sccm of tetrafluoromethane (CF_4), 45 sccm of fluoroform (CHF_3), and 150 sccm of argon at a pressure of 200 mTorr and radio frequency power of 300 W.

Nanostructures Transfer to the PDMS and UV Curable Resin. The nanotemplate were C_4F_8 plasma-treated with 5 sccm of helium and 2 sccm of C_4F_8 at radio frequency power of 150 W and then dehydrated at 150 °C for 1 h. PDMS (Sylgard184; Dow Corning, 10:1 prepolymer/curing agent) membrane was prepared by spin-coating at 500 rpm for 5 s and 1,200 rpm for 30 s on to the substrates and thermally cured at 150 °C for 30 min on a hot plate. The thin PDMS membrane was permanently bonded with a thick PDMS slab after oxygen plasma treatment (270 W, 15 s) and then released from the nano-template. The lens template was prepared by deforming the thin PDMS membrane under a negative pressure drop. The lens curvatures were controlled by changing the pressure drops (7, 13, 20, and 30 kPa). A UV-curable optical resin (NOA 63; Norland Products) recast the curved PDMS membrane with nanostructures under UV exposure of 4.5 J/cm^2.

Measurement for LED Lens Transmission. The lens transmission was measured by using an integrating sphere and spectrometer coupled with a single LED chip (full-width at half-maximum: 120 °, luminous flux: ∼2 lm) of a constant LED emitting angle of 60°, which was determined by precisely controlling the distance between LED chip and the aperture. The aperture size is 2.5 mm in diameter and the distance is about 2 mm for the measured emitting angle of 60°. Transmission of all of the lenses was measured by using this experimental set-up to avoid the measurement error due to the time variation of an LED chip and flux variation between different LED chips. Flux of the LED chip was measured every time after the flux measurement through the LED lens because of time variation (0.006%/min) of the LED chip. A single LED chip was used because different LED chips may have some variation in flux. All of the transmittance values were averaged after three time measurements within the SD of 0.0014 in Fig. 3 and 0.0013 in Fig. 4. Each value excludes light reflection on the bottom surface of the LED lens.

1. Meister R, Hallé MA, Dumoulin H, Pieranski P (1996) Structure of the cholesteric focal conic domains at the free surface. *Phys Rev E Stat Phys Plasmas Fluids Relat Interdiscip Topics* 54(4):3771–3782.
2. De Silva L, et al. (2005) Natural and nanoengineered chiral reflectors: Structural color of Manuka beetles and Titania coatings. *Electromagnetics* 25(5):391–408.
3. Sharma V, Crne M, Park JO, Srinivasarao M (2009) Structural origin of circularly polarized iridescence in jeweled beetles. *Science* 325(5939):449–451.
4. Ghiradel H, Eisner T, Silbergl R, Aneshans D, Hinton HE (1972) Ultraviolet reflection of a male butterfly—Interference color caused by thin-layer elaboration of wing scales. *Science* 178(4066):1214–1217.
5. Saito A, et al. (2006) Reproduction of the Morpho blue by nanocasting lithography. *J Vac Sci Technol B* 24(6):3248–3251.
6. Watanabe K, et al. (2005) Optical measurement and fabrication from a Morpho-butterfly-scale quasistructure by focused ion beam chemical vapor deposition. *J Vac Sci Technol B* 23(2):570–574.
7. Martin-Palma RJ, Pantano CG, Lakhtakia A (2008) Biomimetization of butterfly wings by the conformal-evaporated-film-by-rotation technique for photonics. *Appl Phys Lett* 93(8):083901.
8. Silver J, Withnall R, Ireland TG, Fern GR, Zhang S (2008) Light-emitting nanocasts formed from bio-templates: FESEM and cathodoluminescent imaging studies of butterfly scale replicas. *Nanotechnology* 19(9):095302.
9. Parker AR, Hegedus Z, Watts RA (1998) Solar-absorber antireflector on the eye of an Eocene fly (45 Ma). *P Roy Soc Lond B Bio* 265(1398):811–815.
10. Stavenga DG, Foletti S, Palasantzas G, Arikawa K (2006) Light on the moth-eye corneal nipple array of butterflies. *Proc Biol Sci* 273(1587):661–667.
11. Clapham PB, Hutley MC (1973) Reduction of lens reflection by moth eye principle. *Nature* 244(5414):281–282.
12. Boden SA, Bagnall DM (2008) Tunable reflection minima of nanostructured antire-flective surfaces. *Appl Phys Lett* 93(13):133108.
13. Huang YF, et al. (2007) Improved broadband and quasi-omnidirectional anti-re-flection properties with biomimetic silicon nanostructures. *Nat Nanotechnol* 2(12):770–774.
14. Hong SH, et al. (2009) Imprinted moth-eye antireflection patterns on glass substrate. *Electron Mater Lett* 5(1):39–42.
15. Zhang G, Zhang J, Xie G, Liu Z, Shao H (2006) Cicada wings: A stamp from nature for nanoimprint lithography. *Small* 2(12):1440–1443.
16. Xie GY, et al. (2008) The fabrication of subwavelength anti-reflective nanostructures using a bio-template. *Nanotechnology* 19(9):095605.
17. Beams HW, Anderson E (1955) Light and electron microscope studies on the light organ of the firefly (*Photinus pyralis*). *Biol Bull* 109:375–393.
18. Lee DW, Boo KS (1991) Studies on the light organ of the firefly, *Luciola lateralis* Motschulsky. *Korean J Appl Entomol* 30(1):29–36.
19. Ando Y, et al. (2008) Firefly bioluminescence quantum yield and colour change by pH-sensitive green emission. *Nat Photonics* 2(1):44–47.
20. Vukusic P, Sambles JR, Lawrence CR, Wootton RJ (1999) Quantified interference and diffraction in single Morpho butterfly scales. *P Roy Soc Lond B Bio* 266(1427):1403–1411.
21. Gaylord TK, Baird WE, Moharam MG (1986) Zero-reflectivity high spatial-frequency rectangular-groove dielectric surface-relief gratings. *Appl Opt* 25(24):4562–4567.
22. Smith DS (1963) The organization and innervation of the luminescent organ in a firefly, *Photuris pennsylvanica* (Coleoptera). *J Cell Biol* 16(2):323–359.
23. Schmid H, Michel B (2000) Siloxane polymers for high-resolution, high-accuracy soft lithography. *Macromolecules* 33(8):3042–3049.
24. Chattopadhyay S, et al. (2010) Anti-reflecting and photonic nanostructures. *Mater Sci Eng Rep* 69(1–3):1–35.